

## Influence of Nitrogen Doping on the Defect Formation and Surface Properties of TiO<sub>2</sub> Rutile and Anatase

Matthias Batzill, Erie H. Morales, and Ulrike Diebold

Department of Physics, Tulane University, New Orleans, Louisiana 70118, USA

(Received 25 July 2005; published 20 January 2006)

Nitrogen doping-induced changes in the electronic properties, defect formation, and surface structure of TiO<sub>2</sub> rutile(110) and anatase(101) single crystals were investigated. No band gap narrowing is observed, but N doping induces localized N 2*p* states within the band gap just above the valence band. N is present in a N(III) valence state, which facilitates the formation of oxygen vacancies and Ti 3*d* band gap states at elevated temperatures. The increased O vacancy formation triggers the 1 × 2 reconstruction of the rutile (110) surface. This thermal instability may degrade the catalyst during applications.

DOI: 10.1103/PhysRevLett.96.026103

PACS numbers: 68.35.-p, 81.05.Je, 82.65.+r

Titanium dioxide (TiO<sub>2</sub>) is a good photocatalyst for the remediation of organic pollutants and the photogeneration of hydrogen from water [1–3]. Unfortunately, TiO<sub>2</sub> has a wide band gap, which limits its photoactivity to ultraviolet light. To utilize a wider range of the solar spectrum, the band gap needs to be narrowed. Recently, it has been suggested that this can best be achieved by replacing lattice oxygen with appropriate anion dopants, particularly nitrogen [4]. Here we describe the fundamental changes that are induced in the surface electronic and geometric structure by introducing N into the TiO<sub>2</sub> lattice. Dopant-induced lowering of the O vacancy formation energy causes a restructuring of the rutile surface. This unexpected phenomenon may be relevant for many doped oxide systems.

Dopant-induced energy levels within the band gap may increase the yield for electron-hole pair formation under illumination with visible light. The traditionally used transition metal doping of TiO<sub>2</sub> suffers from thermal instabilities and the formation of carrier recombination centers due to strongly localized states within the band gap [5,6]. Similarly, Ti 3*d* states, which form as the consequence of reduction of Ti<sup>4+</sup> to Ti<sup>3+</sup>, cause shallow defect states that trap holes and, thus, are also counterproductive for hole-related photocatalytic processes [7]. Based on density-functional theory (DFT) calculations, Asahi *et al.* [4] proposed substituting oxygen with anions, in particular, nitrogen, as a better approach. Hybridization of N 2*p* states with the O 2*p*-derived valence band is supposed to achieve a band gap narrowing. Optical absorption studies on N-doped TiO<sub>2</sub> indicate a gap narrowing [4,8], but absorption due to localized N states and Ti<sup>3+</sup> defect states may also contribute to this effect [9]. Recent DFT calculations indicate *no* band gap narrowing due to N doping but rather that N 2*p* states form localized states within the band gap just above the valence band maximum [10,11]. Furthermore, N doping, possibly, affects the anatase and rutile polymorphs differently [10]. Some of the discrepancies and ambiguities in experimental observations may arise from challenges in preparing well-defined samples. Typical photocatalysts are complex nanoscale materials that are

not easily characterized at the atomic scale. By investigating well-characterized model systems under controlled conditions, we can isolate surface effects that are brought about by introducing N into the TiO<sub>2</sub> lattice.

The anatase sample, a natural mineral, was initially yellowish/transparent and turned blue upon vacuum annealing. X-ray photoelectron spectroscopy (XPS), scanning tunneling microscopy (STM), and low energy ion scattering spectroscopy did not detect any impurities after a few cycles of sputtering and annealing. A commercial, epipolished rutile sample (MTI Corporation) was used. STM, XPS, and UV-photoelectron spectroscopy (UPS) studies were performed in separate ultrahigh vacuum (UHV) chambers. Empty-state STM images were obtained with a bias voltage of 1–2 V. Angle resolved UPS was performed at the 3 m toroidal grating monochromator synchrotron beam line at the Center for Advanced Microstructures and Devices, Baton Rouge, Louisiana. The data were collected in normal emission with the incident light at 45°. The single crystalline rutile (110) and anatase (101) samples were doped by low energy (1 keV) N ion implantation with an ion fluence of ~10<sup>15</sup> ions/cm<sup>2</sup>. Under these conditions, binary collision simulations indicate a mean implantation depth of 3.1 nm for rutile TiO<sub>2</sub> [12].

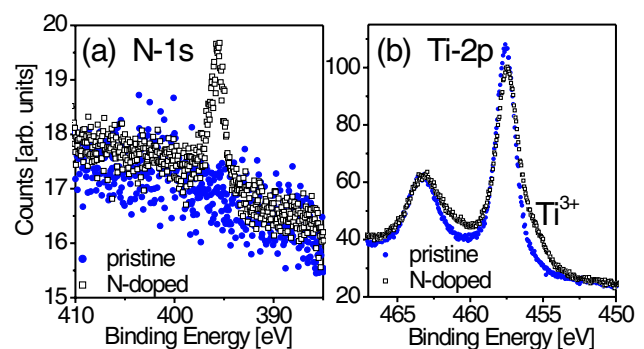


FIG. 1 (color online). XPS of pristine (undoped) and N-doped and annealed rutile-TiO<sub>2</sub>.

The XPS data in Fig. 1, excited with an  $AlK\alpha$  x-ray source, show a single N  $1s$  peak at  $\sim 396$  eV binding energy; from the N  $1s$  to O  $1s$  peak ratio, we estimate an N concentration of  $\sim 3\%$  as the average concentration in the sampling depth of the XPS measurement. The N  $1s$  peak position is indicative of a  $N^{3-}$  species. The measured binding energy (BE) is, however, even lower than that of titanium nitride, suggesting more charge transfer to the nitrogen. Such a BE has been reported for titanium oxynitrides [13] and is thus consistent with the formation of substitutional, diluted  $N^{3-}$  dopants in a  $TiO_2$  matrix. Angle resolved XPS shows very similar photoelectron diffraction effects for the N  $1s$  as for the O  $1s$  signal, indicating substitutional replacement of O by N. The intensity of this N  $1s$  peak was correlated to the increased visible light-photoactivity of  $TiO_2$  by Asahi *et al.* [4]. When we vacuum anneal N-doped  $TiO_2$ , the N  $1s$  peak shape and intensity is unchanged, while the Ti  $2p$  line is significantly altered for both polymorphs with a shoulder indicative of  $Ti^{3+}$ . Figure 1(b) shows the XPS spectra for rutile.

An exact knowledge of the electronic states is important for understanding the modifications that result from N doping; these were probed with UPS; see Fig. 2. The clean rutile (110) sample exhibits the characteristic Ti  $3d$ -derived gap state that is attributed to a few percent of surface oxygen vacancies [14] [see also inset in Fig. 2(a)]. The anatase (101) surface reduces not as easily and exhibits a less intense Ti  $3d$  gap state [15]. Exposure of the surfaces to  $\sim 100$  langmuirs  $O_2$  completely quenches these gap states. Interestingly, N implantation at room temperature *also* decreases the Ti  $3d$  gap state intensity (Fig. 2) in both samples. However, their intensity increases again after subsequent annealing in UHV. For N-doped anatase

(101), the Ti  $3d$  gap state becomes even more intense than for the undoped sample.

The O  $2p$ -derived valence band maximum appears unchanged in UPS after N implantation. However, additional states within the band gap directly on top of the valence band form after N doping [Fig. 2(a)]. The small intensity of these additional states compared with the mainly O  $2p$ -derived valence band (VB) suggests that these states may be *localized* N  $2p$  states. Thus, *no* band gap narrowing due to a uniform shift of the entire VB maximum to lower binding energies is observed as was asserted by Asahi *et al.* [4]; instead, our observations support more recent DFT calculations [10,11]. For rutile, the N  $2p$  states extend about  $\sim 0.4$  eV into the band gap from the VB maximum. This estimate has been obtained by subtraction of the normalized UPS spectrum of the pristine sample from that of the N-doped sample and by subsequently assessing the intensity of this difference spectrum in the band gap region of undoped  $TiO_2$ . For anatase, similar N  $2p$  states are observed after room temperature N doping [Fig. 2(b)]. After annealing of the anatase sample, the N-derived states span the region in the band gap from the VB-maximum up to the higher lying Ti  $3d$  defect states [Fig. 2(c)]. This implies that the N-induced state span a wider energy range for anatase than rutile.

In order to discriminate between N  $2p$  and Ti  $3d$  band gap states and, thus, to ascertain that the observed band gap states are indeed a consequence of the N doping, resonant photoemission data were collected [Fig. 2(d)]. The intensity of Ti-derived states exhibit a maximum around 50 eV photon energy [14,16,17], which is observed for the upper ( $\sim 0.87$  eV) but not the lower ( $\sim 2.2$  eV) lying band gap states in Fig. 2(d). Furthermore, only the higher lying states (0.87 eV) are quenched upon exposure to oxygen. These two observations indicate that only the upper band gap states are Ti-derived, and the lower states are indeed N  $2p$  as discussed in the previous paragraph.

In the photon-energy range used in UPS (35–110 eV), the measurements are extremely surface sensitive. Thus, the unchanged N  $2p$  component for rutile before and after sample annealing [Fig. 2(a)] implies *no* surface segregation or even desorption of implanted N. The somewhat increased N component for anatase [Fig. 2(b)], on the other hand, could indicate N diffusing to the surface. In XPS ( $AlK\alpha$ ), a somewhat deeper sampling depth is obtained, and no significant change of the N concentration before and after annealing was measured for both polymorphs, indicating that no noteworthy amount of N is desorbed.

The long-range order observed in low energy electron diffraction disappears only for N concentrations exceeding  $\sim 6\%$ . Nitrogen doping and subsequent annealing has a distinct effect on the *local* surface structure; see Fig. 3. Especially for rutile (110), STM reveals an unexpected effect. The typical  $1 \times 1$  surface of pristine rutile (110) [Fig. 3(a)] exhibits additional domains of bright stripes

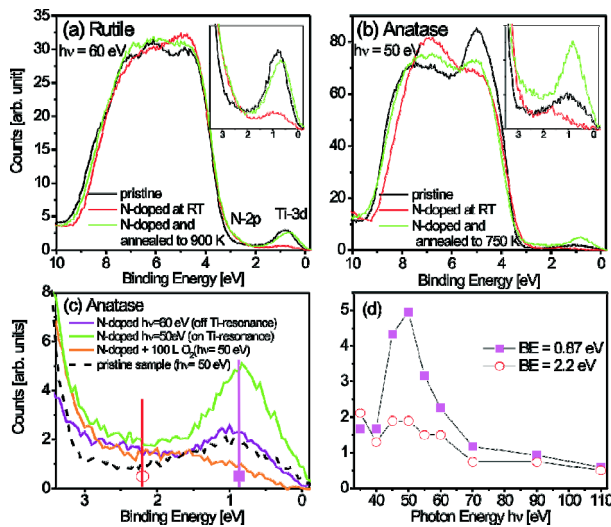


FIG. 2 (color online). UPS spectra of undoped (pristine) and N-doped  $TiO_2$  after room temperature N implantation and annealing for (a) rutile (110) and (b) anatase (101). The band gap region of anatase is magnified in (c), and the photon-energy dependence of two gap state features displayed in (d).

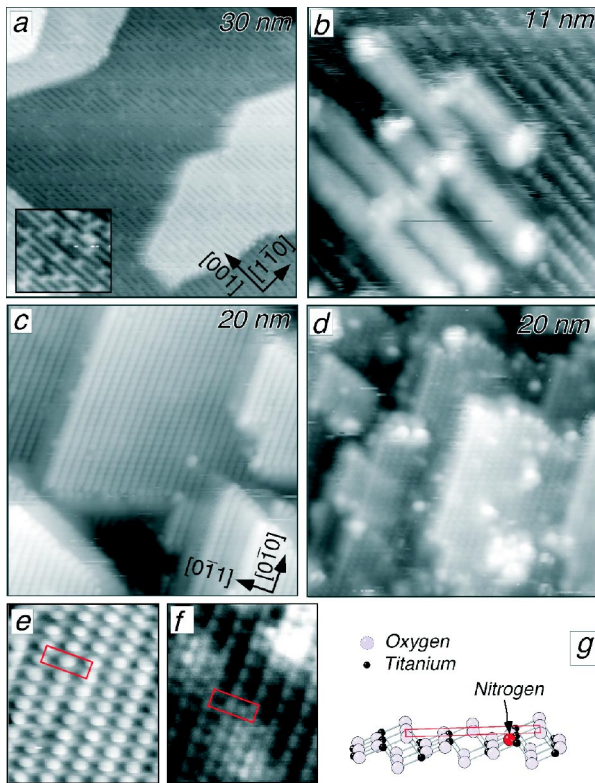


FIG. 3 (color online). STM images of rutile, (a) pristine and (b) after N implantation and vacuum annealing, and anatase (101) (c),(e) pristine and (d),(f) N implanted/annealed. In (e), (f), and (g), the unit cell is indicated. In the high resolution STM images, the bright protrusions are assigned to the bridging twofold oxygen atoms. The model in (g) shows an anatase (101) surface with the potential position of a surface N dopant atom.

after ion implantation and annealing [Fig. 3(b)]. In STM, the stripes exhibit the same structure as the well-known  $1 \times 2$  reconstruction that is usually only observed for strongly reduced  $\text{TiO}_2$  crystals [14].

The density of the reconstructed areas scales with the N dosage, and the reconstruction disappears upon removal of the N-doped surface layer by Ar sputtering. The  $(1 \times 1)$  structure of the anatase (101) surface [Fig. 3(c)] exhibits nanosized protrusions after N implantation/annealing. The bigger and brighter features in the STM image in Fig. 3(d) are possibly attributed to oxygen-deficient areas that are disordered. In addition, atomic-size defects are discerned in atomically resolved images. Figure 3(e) shows an STM image of a pristine surface; such surfaces exhibit almost no defects. After N doping and annealing, many atomic features appear brighter [Fig. 3(f)] on the otherwise unchanged atomic configuration. These features are tentatively associated with electronic variations in the local empty electronic states due to substitutional N atoms and/or neighboring reduced Ti sites as indicated in the ball-and-stick model in Fig. 3(g).

From these experimental findings, we reach the following conclusions: N doping results in no band gap narrow-

ing, but instead  $N 2p$  states form within the band gap close to the valence band maximum. The associated changes in the electronic and geometric surface structure can simply be attributed to  $N^{3-}$  substituting lattice  $O^{2-}$ . Ion implantation introduces N that, in order to obtain its preferred 3-state, oxidizes  $Ti^{3+}$  surface species to  $4+$ . This causes the suppression of the Ti 3d band gap states and, thus, the removal of trapping centers for photogenerated holes. However, annealing of the sample *reverses* this effect, and an *increase* in the Ti 3d defect state is observed. We propose that this is because charge neutrality requires that substitutional  $N^{3-}$  species are compensated by oxygen vacancies; these are easily formed by heating—in agreement with recent calculations that predict a drastic reduction in the oxygen vacancy formation energy in N-doped anatase [18]. The accompanying reduction of Ti atoms to  $3+$  gives rise to the intense Ti 3d-derived gap state in UPS (Fig. 2). A completely unexpected, but potentially important, effect is the change of surface structure by the N facilitated oxygen vacancy formation; in rutile (110), it causes a restructuring to  $1 \times 2$ -type domains. In undoped rutile (110), a high oxygen vacancy concentration is necessary for this reconstruction to form, implying that N dramatically increases the chemical potential for oxygen vacancies. The formation of a surface reconstruction indicates that the oxygen vacancies are not bound to the direct vicinity of the N dopant atoms but are mobile. Consequently, compensation of charges may be achieved over long distances. A long-range charge compensation is also in agreement with the quenching of the Ti 3d state by room temperature N implantation.

These results are significant, as they imply that the benefits of N doping come with the prize of thermal instability of the catalyst, which causes increased oxygen vacancy formation. The Ti 3d gap states associated with O vacancies may act as hole trapping sites and, thus, degrade the photocatalyst. Nitrogen doping also causes a substantial surface restructuring, which can seriously affect photocatalytic surface processes.

Other dopants also increase the O vacancy concentration in  $\text{TiO}_2$ , and, thus, it may be projected that a surface restructuring of doped  $\text{TiO}_2$  could be observed for many other systems. For instance, in the dilute ferromagnet, Co-doped  $\text{TiO}_2$ , O vacancies are formed to compensate for the Co charge [19], and, incidentally, these O vacancies are believed to play an important role in explaining the coupling of the magnetic moments in all dilute ferromagnetic oxides [20]. Future studies will show if the here-reported phenomenon of N-induced surface reconstruction is a general trend for other doped  $\text{TiO}_2$  systems.

The authors acknowledge fruitful discussions with Professor Selloni, Dr. Gong (Princeton University), Dr. Di Valentin (Università degli Studi di Milano-Bicocca), and Professor Garfunkel (Rutgers University). Financial support from DOE (DE-TG02-05ER15702), NSF, and NASA is acknowledged.

- [1] A. Mills and S. Le Hunt, *J. Photochem. Photobiol., A* **108**, 1 (1997).
- [2] B. O'Regan and M. Grätzel, *Nature (London)* **353**, 737 (1991).
- [3] A. Fujishima and K. Honda, *Nature (London)* **238**, 37 (1972).
- [4] R. Asahi, T. Morikawa, T. Ohwaki, K. Aoki, and Y. Taga, *Science* **293**, 269 (2001).
- [5] A. K. Gosh and H. P. Maruska, *J. Electrochem. Soc.* **124**, 1516 (1977).
- [6] W. Choi, A. Termin, and M. R. Hoffmann, *J. Phys. Chem.* **98**, 13 669 (1994), and references therein.
- [7] M. A. Henderson, J. M. White, H. Uetsuka, and H. Onishi, *J. Am. Chem. Soc.* **125**, 14 974 (2003).
- [8] H. Irie, Y. Watanabe, and K. Hashimoto, *J. Phys. Chem. B* **107**, 5483 (2003).
- [9] Y. Nakano, T. Morikawa, T. Ohwaki, and Y. Taga, *Appl. Phys. Lett.* **86**, 132104 (2005).
- [10] C. Di Valentin, G. Pacchioni, and A. Selloni, *Phys. Rev. B* **70**, 085116 (2004).
- [11] J. Y. Lee, J. Park, and J.-H. Cho, *Appl. Phys. Lett.* **87**, 011904 (2005).
- [12] The implantation depth was calculated for an amorphous substrate with the density and composition of TiO<sub>2</sub> using the stopping and range of ions in matter (SRIM) code available at <http://www.srim.org>.
- [13] F. Esaka *et al.*, *J. Vac. Sci. Technol. A* **15**, 2521 (1997).
- [14] U. Diebold, *Surf. Sci. Rep.* **48**, 53 (2003).
- [15] W. Hebenstreit, N. Ruzycki, G. S. Herman, and U. Diebold, *Phys. Rev. B* **62**, R16 334 (2000).
- [16] J. Nerlov, Q. Ge, and P. J. Møller, *Surf. Sci.* **348**, 28 (1996).
- [17] A. G. Thomas *et al.*, *Phys. Rev. B* **67**, 035110 (2003).
- [18] C. Di Valentin, G. Pacchioni, A. Selloni, S. Livraghi, and E. Giamello, *J. Phys. Chem. B* **109**, 11 414 (2005).
- [19] J. E. Jaffe, T. C. Droubay, and S. A. Chambers, *J. Appl. Phys.* **97**, 073908 (2005).
- [20] J. M. D. Coey, M. Venkatesan, and C. B. Fitzgerald, *Nat. Mater.* **4**, 173 (2005).